

## EXPERIMENTAL STUDY ON THE PERFORMANCE OF THE RC FRAME INFILLED CAST-IN-PLACE NON- STRUCTURAL RC WALLS RETROFITTED BY USING CARBON FIBER SHEETS

Tomoaki SUGIYAMA<sup>1</sup>, Masahiko UEMURA<sup>2</sup>, Hiroshi FUKUYAMA<sup>3</sup>, Katsuhiko NAKANO<sup>4</sup> And Yasuhiro MATSUZAKI<sup>5</sup>

### SUMMARY

In the past earthquakes, severe damages were observed in RC frames with cast-in-place non-structural RC wall. However, there are no evaluation methods for designing the stiffness and the capacity of this RC frame type. Further no effective techniques are proposed to control the damage level of the cast-in-place non-structural RC walls. This paper describes a shear loading test and a finite element method (FEM) analysis, which were conducted using one-story one-span RC frame specimens with cast-in-place non-structural RC walls to propose an estimation technique. From the test and the analysis, The following conclusion was obtained.

- The initial stiffness of the RC frame with non-structural RC walls was higher than that of a RC frame without wall, and it was similar to that of a RC frame with shear wall. The capacity of the RC frame with cast-in-place non-structural wall was close to the flexural strength of the independent RC frame caused by the failure of non-structural RC walls.
- The FEM analysis is useful method to investigate the shear resistant mechanism of the RC frame with cast-in-place non-structural RC walls, since cracking pattern, failure mode and shear force- deflection characteristics of the tested frames were represented by the analysis.

The seismic retrofit technique using carbon fiber sheets improved the damage level of non-structural RC walls in RC frame. In particular, the deflection of door opening and the residual crack widths can be controlled by retrofitting in carbon fiber sheets.

### INTRODUCTION

In the Japanese conventional cast-in-place reinforced concrete (RC) buildings, RC frames (columns and beams) and the non-structural RC walls (mullion, spandrel and side-wall) were constructed simultaneously, so they were connected rigidly. In the past earthquakes, severe damages were observed in not only RC columns but also cast-in-place non-structural RC walls. When the cast-in-place non-structural RC walls were failed, it became difficult to open the door in the cast-in-place non-structural RC walls, then inhabitants in their room could not take refuge through the doors. Additionally, large shear cracks in cast-in-place non-structural RC walls cause anxious of the inhabitants about the safety of structural member. However, there are no evaluation methods for designing stiffness and capacity of the RC frame with cast-in-place non-structural RC wall, because the change of shear resistant mechanism of with cast-in-place non-structural RC wall was not cleared. Though it has been recommended as the conventional method to use isolation detail (called slit) between cast-in-place non-structural RC walls and RC columns, serious damages were observed in the buildings where the detail of the isolations were not suitable detail [Architectural Institute of Japan, 1997]. Purpose of this paper is as follows:

<sup>1</sup> Department of Architecture, Faculty of Engineering, Science University of Tokyo, Japan Email: j4198620@ed.kagu.sut.ac.jp

<sup>2</sup> Nippon Steel Composite Co. Ltd., Tokyo, Japan Fax: +81-3-5623-5551

<sup>3</sup> Building Research Institute, Tsukuba, Japan Email: fukuyama@kenken.go.jp

<sup>4</sup> Faculty of Engineering, Science University of Tokyo, Tokyo, Japan Email: knakano@rs.kagu.sut.ac.jp

<sup>5</sup> Faculty of Engineering, Science University of Tokyo, Tokyo, Japan Email: ymatsu@rs.kagu.sut.ac.jp

- (1) To obtain results the structural performance of the RC frame with cast-in-place non-structural RC walls from test and analysis.
- (2) To suggest a seismic retrofit technique using carbon fiber sheets for controlling the failure mode of the RC frame with cast-in-place non- structural RC walls .

For above purposes, shear loading tests and analysis of the one-story one-span RC frame with cast-in-place non-structural RC walls were conducted.

## **OUTLINE OF TEST AND ANALYSIS**

### **Specimen**

Details of specimens are shown in Table 1 and Figure 1 (a). Table 2 shows mechanical properties of steel bars and the carbon fiber sheet using the test. The specimen, one-story one-span RC frame with cast-in-place non-structural RC walls, was supposed a frame in the apartment houses. Eight specimens, which were modelled with a scale of 1/3 were prepared (two conventional RC specimens and six strengthen specimens). The column and beam of the frame were unique in all specimens. The cross section of column ( $B_c \times D_c$ ) was 240mm  $\times$  240mm and the thickness of non-structural walls was 40 mm. The length of the non-structural RC wall was 1760mm, and the height was 1100mm. A seismic retrofit using carbon fiber sheet was applied to control the damage level of the non-structural RC walls.

The parameters set in the test were types of openings in the non-structural RC walls and strengthened methods with carbon fiber sheets on the non-structural walls. The A-type opening specimen had a central door opening and two window openings at both side of the door opening in the non-structural RC walls. The B-type opening specimen had two doors openings in it. No.1-4, 7 and 8 were "A-type opening specimen", and No.5 and No.6 were "B-type opening specimen". The No.1 and No.5 were planned conventional RC specimen without carbon fiber sheets.

Table 1 and Figure 1 (b) show the strengthened methods of carbon fiber sheets on the non-structural wall. The parameters of carbon fiber sheets were strengthened area (I-type and L-type), amount of sheets and setting methods of sheets. In I-type strengthened specimen, sheets were set on the mullion walls both side of the door, and in L-type strengthened specimen, sheets were set on both the mullion and the spandrel. The amount of sheets was referred to layers of sheets. One or two layer of sheets were used in this test. The sheets were placed only one side surface of the non-structural walls or both sides. In No.7 and No.8 specimen, the carbon fiber sheets adhered to wall surface by heating the prepreg (resin impregnated) sheets.

### **Method of experiment**

Figure 1(c) shows the loading apparatus. The axial load, kept constant during the test ( $N=B_c \times D_c \times f_c'/6$ ), was applied to specimen by two jacks. The lateral load was applied to the specimen by horizontal jacks on loading beam. The shear cyclic loading was controlled by story drift angle, and the maximum story drift angles ( $R$ ) in cycles were  $\pm 1/6400$ ,  $\pm 1/3200$ ,  $\pm 1/1600$ ,  $\pm 1/800$ ,  $\pm 1/400$ ,  $\pm 1/200$ ,  $\pm 1/100$ ,  $\pm 1/50$ rad. and  $+1/25$ rad. The out-of-plane deflection of specimens were confined by pantographs above the loading beam

### **Finite element method**

The analysis was used to clear the shear resistant mechanism of the RC frame with cast-in-place non-structural RC wall. The mesh layouts of non-structural RC wall specimen are shown in Figure 2. The longitudinal bar in column was represented by line element, and shear reinforcing bars were arranged in two orthogonal directions and placed two layer in each direction. The bond between longitudinal bar and concrete was represented by bond link. In connection of members (columns, beams, and non-structural walls), the crack link was set for crack opening, and the dowel action of reinforcing bar was considered by dowel link. In this representation, the analysis result of the independent frame specimen and the shear wall specimen showed good agreement with the test result [Sugiyama et al, 1998].

## RESULT AND DISCUSSION

### Failure mode in test

The failure mode of the conventional non-structural RC wall specimens (No.1 and No.5) were similar to the observed damage of existing buildings due to earthquakes. The examples of cracking patterns are shown in Figure 3. First, the diagonal cracks were observed from corner of openings in both the A-type specimen (No. 1) and the B-type specimens (No, 5). In the A-type specimen, shear cracks in mullion and spandrel were observed around  $1/800\text{rad}$ . in story drift angle. Finally, the decrease of shear force was caused by the shear failure in mullion and compressive failure of column-spandrel connection concrete. In the B-type specimen, shear cracks and flexural compressive failure of side-wall concrete were observed after first cracks was observed. Next, shear cracks developed along the vertical reinforcing bar in the side-wall. Finally the column and the side-wall slid off vertically, then the decrease of shear force was caused by that.

Cracks of the strengthened specimens were observed from back side of the specimen or by peeling off the sheet after the test, since sheets were placed on the surface of non-structural wall (mullion, spandrel, side-wall). The failure state of the strengthened specimens were similar to that of conventional RC specimens. However in the strengthened specimen, the number of shear cracks increased in strengthened area of non-structural wall, but crack widths were decrease by using carbon fiber sheets. Moreover in A-type specimen, the shear failure of the mullion became the flexural failure by using carbon fiber sheets.

### Deformation properties in test

Figure 4 (a) and (b) show the shear force (Q)- displacement ( $d$ ) relationships of conventional non-structural RC wall specimen (No.1 and 5), and Figure 4 (c) shows the skeleton curve of these specimen, with curves of shear wall specimen (thickness of the wall panel=60mm) and independent frame specimen. The shear wall specimen and the frame specimen were tested in the past research [Horie et al, 1997]. The cross section and the bar arrangement of the column and the beam were the same as that of this test.

The initial stiffness of conventional non-structural wall specimen (No.1 and 5) were higher than that of the frame specimen, and were similar to that of the shear wall specimen. The value of initial stiffness of No.1 and No.5 were equal to 3.4 and 4.5 times larger than that of the frame specimen. Reduction in the stiffness was observed around  $1/800\text{rad}$ . in story drift angle due to the failure of non-structural RC walls (mullion, spandrel, side-wall). After maximum load was observed, the shear force decreased slowly, but it was rather higher than the flexural strength of the frame specimen. Furthermore, the hysteresis of non-structural wall specimens were ductile.

Figure 5 (a) shows skeleton curve of the shear force (Q)- displacement ( $d$ ) relationships of A-type specimen (No.1-4, 7 and 8), and Figure 5 (b) shows Q-  $d$  relationships of B-type specimen (No.6 and 7). In all A-type specimens, reduction of the stiffness was observed when story drift angle ( $R$ ) was within  $1/800\text{rad}$ . -  $1/400\text{rad}$ ., nevertheless, the reduction of stiffness in the strengthened specimens were smaller than that in the conventional specimens. Further in the strengthened specimen, the reduction of stiffness was different by choosing the strengthened method with sheets. Moreover, shear force of strengthened specimens was higher than that of conventional specimen around  $1/200\text{rad}$ . in story drift angle ( $R$ ). In B-type strengthened specimen, same improvements in stiffness and shear force was observed as that of A-type strengthened specimen. After the story drift angle ( $R$ ) was over  $1/100\text{rad}$ ., the curve of strengthened specimen was similar to that of conventional specimens in both A-type and B-type specimen, since the carbon fiber sheets peeled off from the walls, but the hysteresis of strengthen specimens were ductile.

### Analytical result

Figure 3 shows crack patterns of analysis, and Figure 4(d) shows skeleton curve of the shear force(Q)-displacement( $d$ ) relationships skeleton curve of analysis. The shear capacity of FEM analysis was lower than that of test. However, good agreement between the analysis and the test can be seen in Figure 3 in crack propagation and progress of failure. In particular, shear capacity of analysis due to the shear failure of mullion and compressive failure of concrete was the same as the test result. Moreover, skeleton curve of Q- $d$  relationships by analytisis agree with that of test result, and analytical result indicated that the decrease of stiffness was caused to failures of non-structural RC wall in the RC frame. Thus, analytical method is useful to clear the shear resistant mechanism of a RC frame with cast-in-place non-structural RC walls.

## Improvement by sheets

To control the deformation of door opening and crack widths are required, so deflection angles of door opening and residual crack width of non-structural walls were discussed.

### *Deflection angle of door opening*

Figure 6 (a) and (b) show average shear stress ( $t_0$ ) – deflection angle of door opening ( $R_D$ ) relationships (Figure 6 (a) shows A-type specimen, Figure 6 (b) shows B-type specimen). The shear force divided by minimum horizontal section equal to the average shear stress ( $t_0$ ). The shear stress  $f_{ss}$  in Figure 6 is allowable shear stress for temporary loading in “Standard for Structural Calculation of Reinforced Concrete Structures” [Architectural Institute of Japan (AIJ), 1988; revised in 1991]. It is a limit for shear stress level when middle level earthquake happen (80-100 gal). In both A-type specimen and B-type specimen, the deflection angle of door opening differed between the strengthened specimen and conventional RC specimen beyond the stress level of  $f_{ss}(=1.09 \text{ N/mm}^2)$ . In strengthened specimen the decrease of stiffness was smaller in order of I-type 1-layer, I-type 2-layer, L-type 1-layer, L-type 2-layer.

Since the deflection angle of door openings when the door cannot operate is supposed  $1/300$ - $1/100$ rad. [AIJ, 1985], the shear stress in case of  $R_D = 1/300$ rad. and  $1/150$ rad. was discussed. Figure 7 shows the ratio of the average shear stress of strengthened specimen to that of conventional RC specimen. In  $R_D = 1/300$ rad., the ratio of I-type strengthened specimen was within 1.03-1.11, and the ratio of the L-type strengthened specimen was within 1.12-1.13. In  $R_D = 1/150$ rad., the ratio of I-type strengthened specimen was within 1.05-1.13, and the ratio of the L-type strengthened specimen was within 1.20-1.22. Consequently, the shear stress was controlled by choosing strengthen method with sheets when the deflection angle of door opening reached limit angle ( $1/300$ rad. or  $1/150$ rad.).

### *Residual crack width*

After earthquake, the residual cracks caused many problems, so the residual crack widths were discussed. Figure 8 (a) and (b) shows the residual cracks width ( $W$ ) – maximum story drift angles in the cycle ( $R$ ) relationships. The positions of the discussed shear cracks were shown in Figure 8; the shear crack of A-type was in mullion, and that of B-type was in side-wall.

The allowable width of crack is 0.15mm-0.30mm from the view of serviceability and durability [AIJ, 1990]. Thus, when the residual crack widths was over 0.2mm, the story drift angle in the cycle was refer to limit story drift angle. The limit story drift angle was  $1/400$ rad. in A-type specimen, and it was  $1/200$ rad. in B-type strengthen specimen, respectively. The limited deflection angle of strengthened specimen much differed from that of conventional RC specimen, but the limit deflection angle did not differ in parameters of sheets. However, the residual crack widths were smaller in order of I-type 1-layer (No.2), I-type 2-layer (No.3), L-type 1-layer (No.4). Consequently, the residual crack width was controlled by choosing strengthen method with sheets.

## CONCLUSION

- (1) The initial stiffness of the RC frame with non-structural RC walls was higher than that of a RC frame without wall, and it was similar that of frame with shear wall. The capacity of the RC frame with cast-in-place non-structural wall was close to the flexural strength of the independent RC frame caused by the failure of non-structural RC walls.
- (2) The FEM analysis is useful method to investigate the shear resistant mechanism of the RC frame with cast-in-place non-structural RC walls, since cracking pattern, failure mode and shear force- deflection characteristics of the tested frames were represented by the analysis.
- (3) The seismic retrofit technique using carbon fiber sheets improved the damage level of non-structural RC walls in RC frame. In particular, the deflection of door opening and the residual crack widths can be controlled by retrofitting in carbon fiber sheets.

## REFERENCES

- Architectural Institute of Japan (1990), *Principal Guide for Service Life Planning of Building*, AIJ, Tokyo (in Japanese)
- Architectural Institute of Japan (1985), *Recommendations for A Seismic Design and Construction of Nonstructural Elements*, AIJ, Tokyo (in Japanese)
- Architectural Institute of Japan (1997), *Report on the Hanshin-Awaji Earthquake Disaster, Building Series Volume, Structural Damage to Reinforced Concrete Building*, AIJ, Tokyo
- Architectural Institute of Japan (1988; revised in 1991), *Standard for Structural Calculation of Reinforced Concrete Structures*, AIJ, Tokyo
- Horie, K., et al. (1997), "A Study on Retrofitting of Shear Wall with Continuous Fiber Sheet", *Summaries of Technical Papers of Annual Meeting of AIJ*, C-2, pp595-600 (in Japanese)
- Sugiyama, T., et al. (1998), "Analytical study on Shearing Resistant Mechanisms of Reinforced Concrete Shear Wall", *Summaries of Technical Papers of Annual Meeting of AIJ*, C-2, pp811-812 (in Japanese)

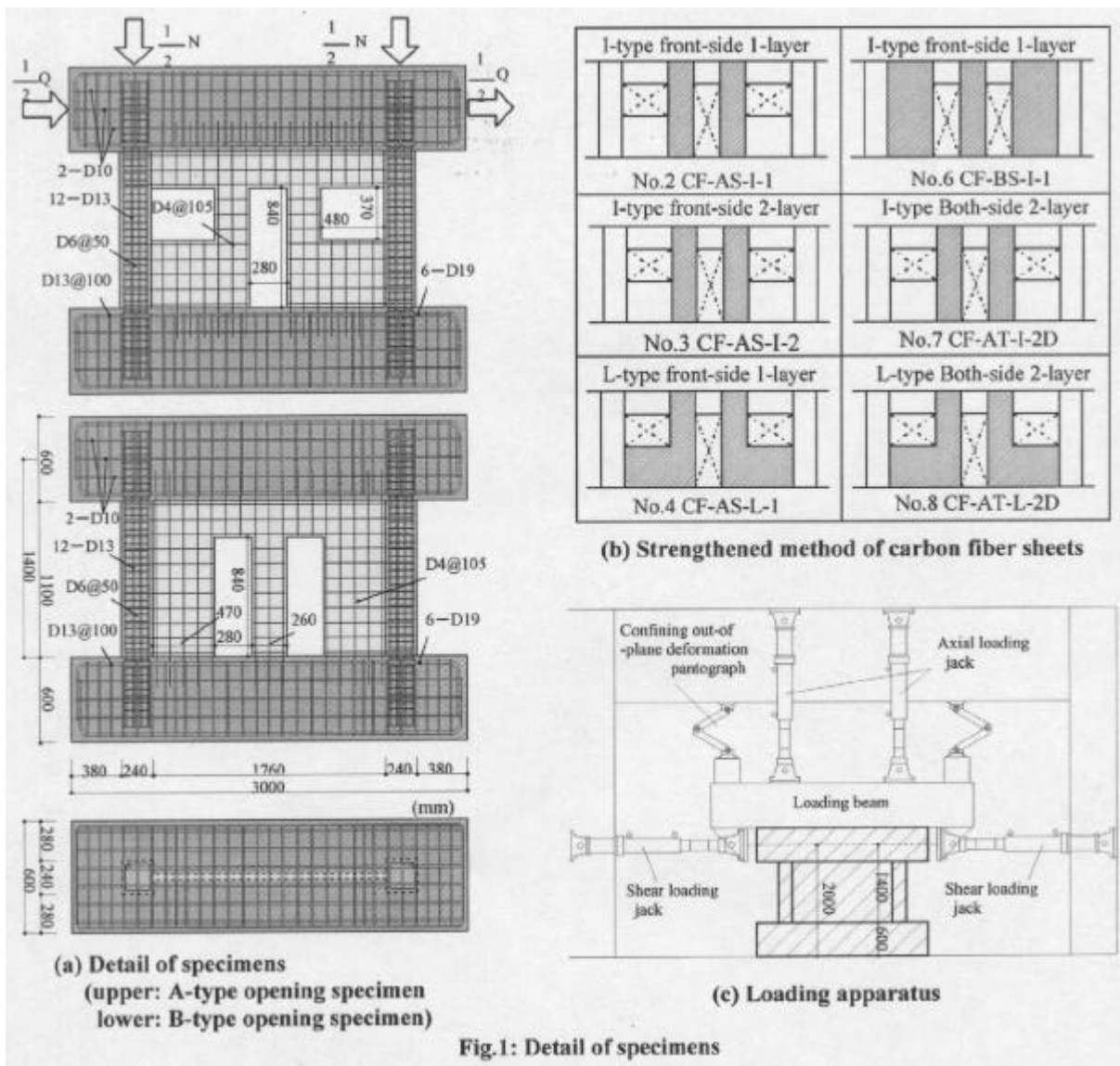
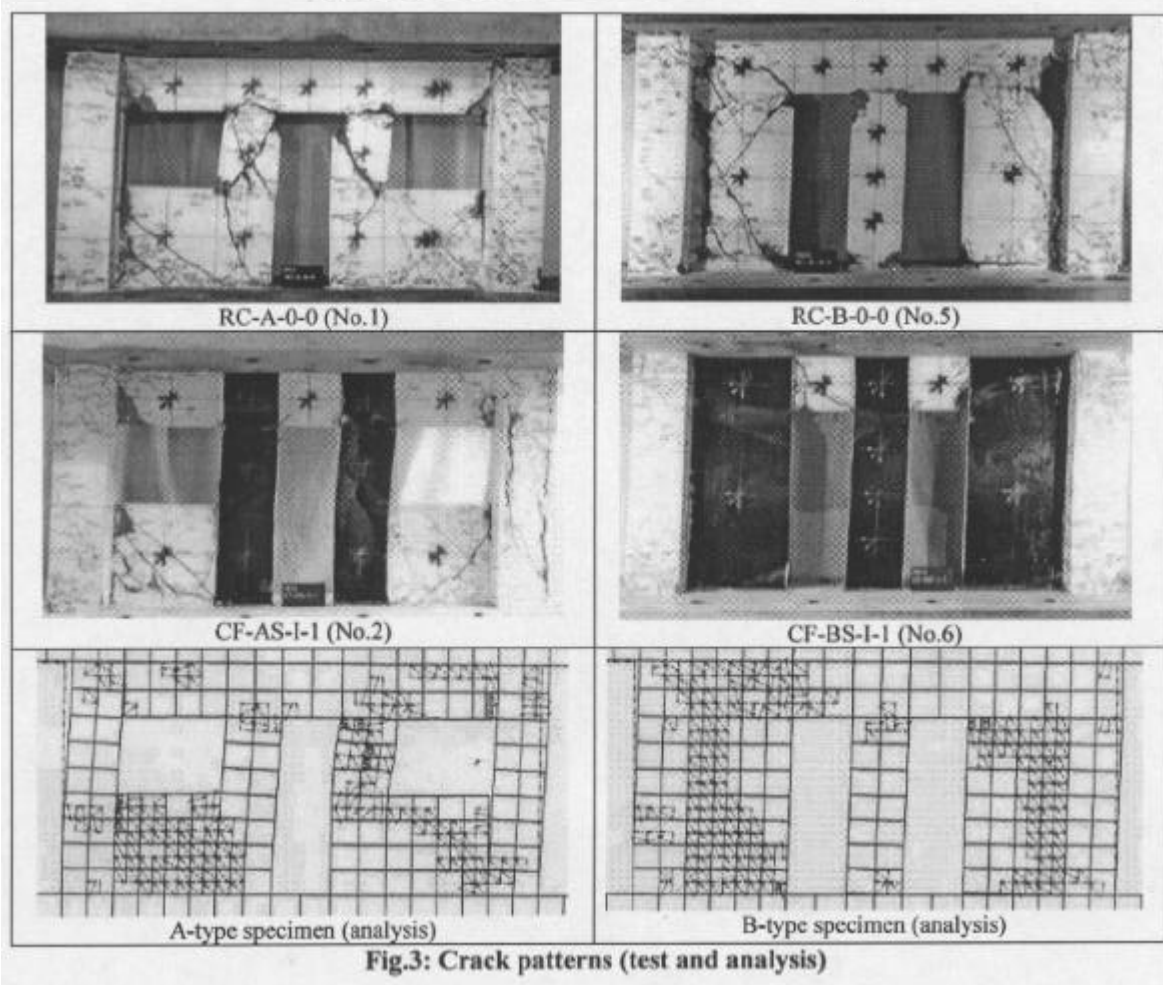
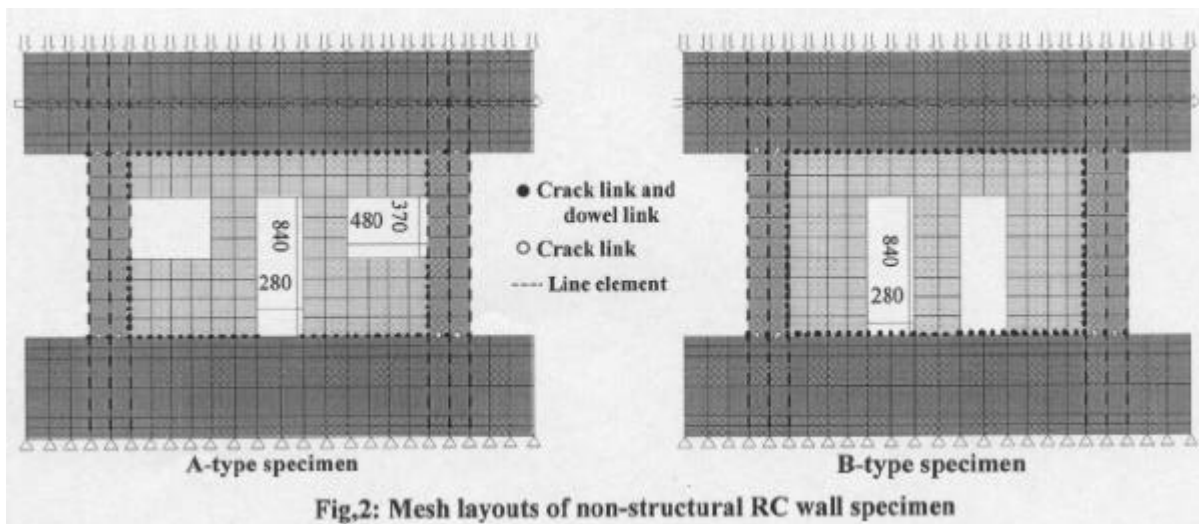
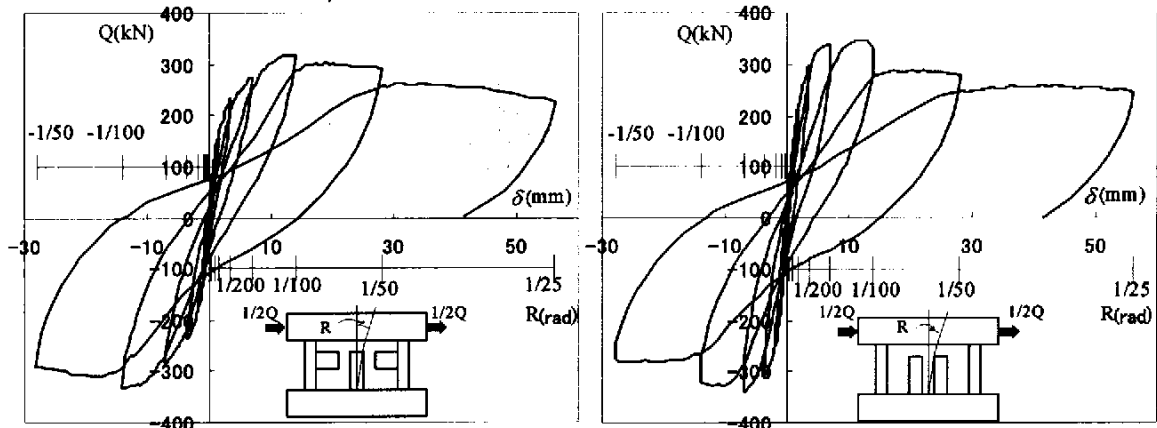


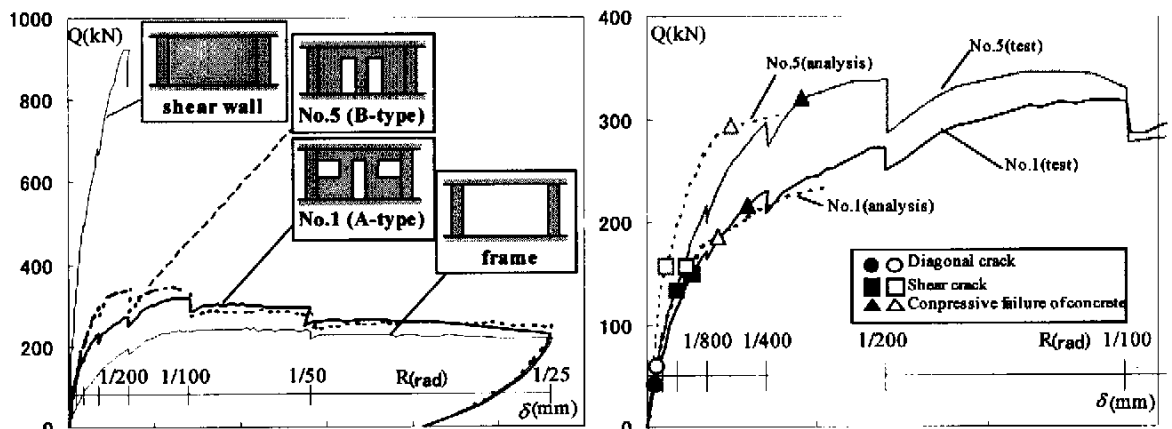
Fig.1: Detail of specimens





(a) A-type opening specimen(No.1)  
Shear force(Q) -Displacement( $\delta$ ) relationship

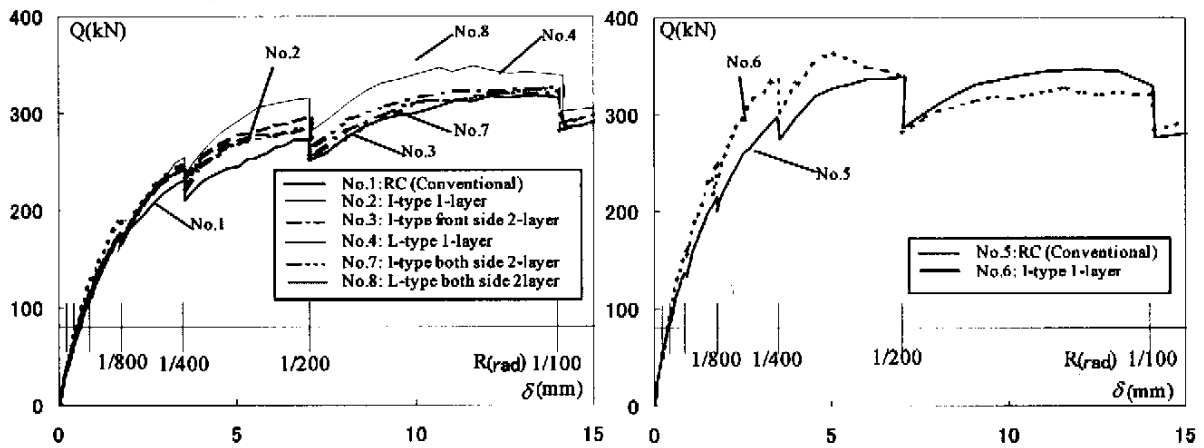
(b) B-type opening specimen(No.5)  
Shear force(Q) -Displacement( $\delta$ ) relationship



(c) Skeleton curve of shear force(Q) -displacement( $\delta$ ) relationship

(d) Skeleton curve of shear force(Q) -displacement( $\delta$ ) relationship in test and analysis

Fig.4: Shear force(Q)-Displacement( $\delta$ ) relationship skeleton curve



(a) A-type opening specimen

(b) B-type opening specimen

Fig.5: Shear force(Q)-Displacement( $\delta$ ) relationship skeleton curve

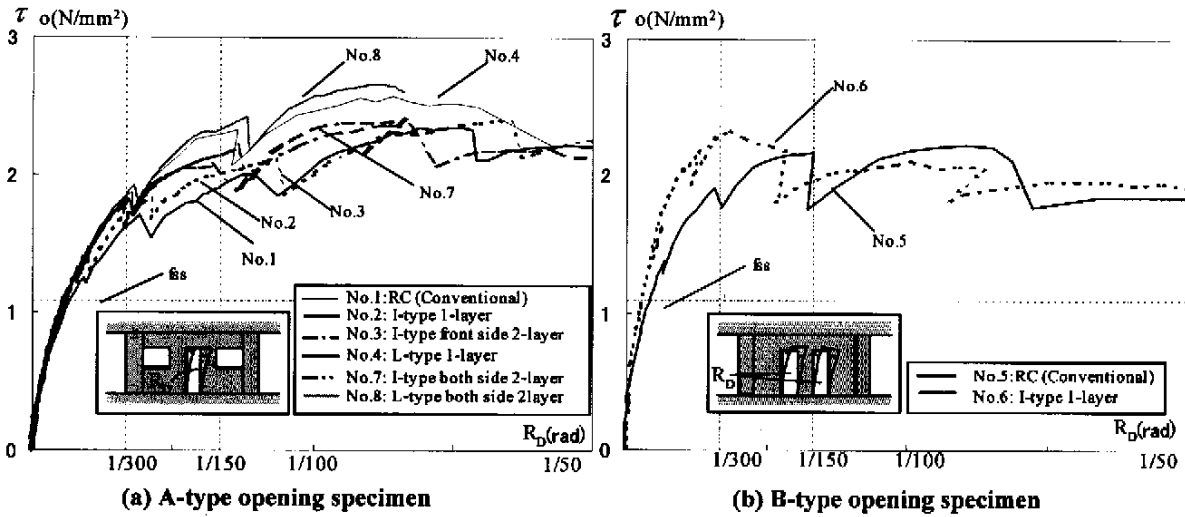


Fig.6 Average Shear Stress( $\tau_o$ )-Deflection angle of door opening( $R_D$ ) relationship skeleton

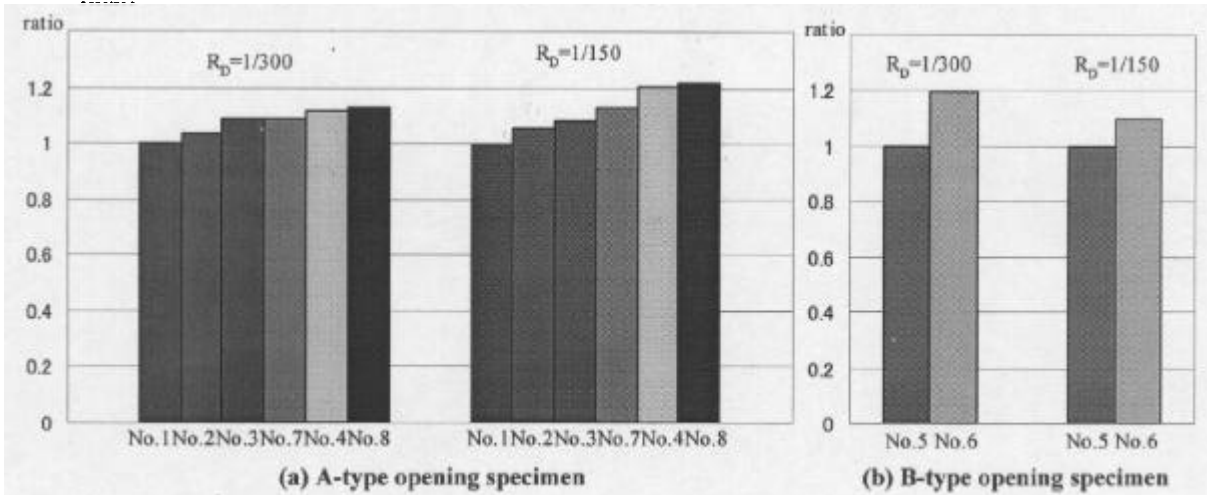


Fig.7: Ratio of the Average Shear Stress of the specimen strengthened to that of conventional RC specimen

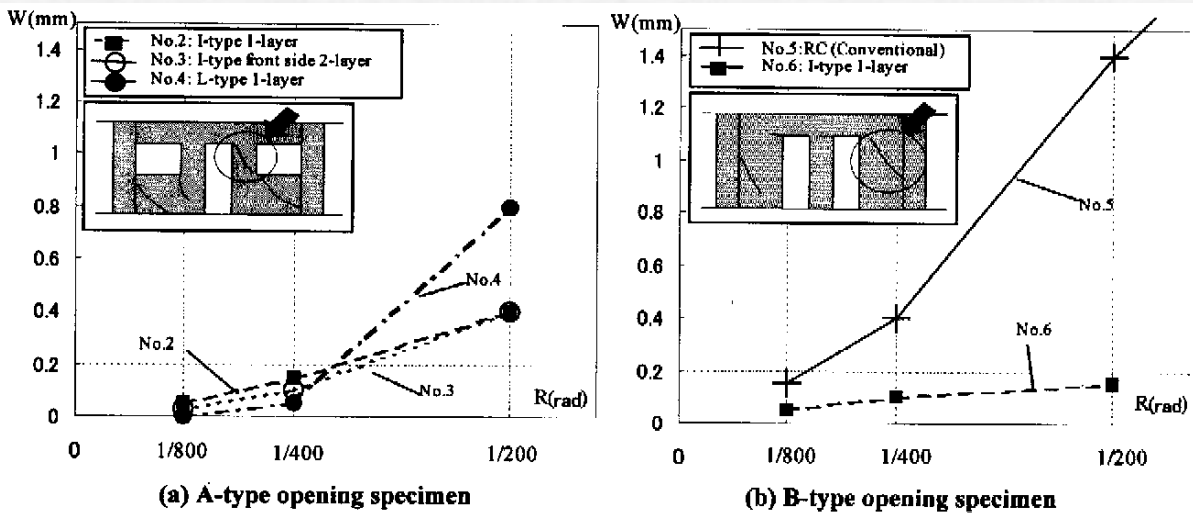


Fig.8: Width of crack in off shear load ( $W$ ) - Deflection angle relationship

The positions of the discussed shear cracks were shown in Figure 8; the shear crack of A-type was in mullion, and that of B-type was in side-wall.